SUPPLEMENTARY METHODS AND FIGURES:

Real-time RT-PCR. Total RNA was extracted from cells with RNeasy mini kit (Qiagen, Valencia, CA). Thirty ng of total RNA was used in a 20-µl reaction of one-step real-time quantitative PCR, using iScript one-step RT-PCR kit for probes (BioRad), and each reaction was run in triplicate in an Eppendorf Realplex PCR machine (Model 5341). TaqMan probes for CD133, DLL1, GFAP, and ACTB were purchased from Applied Biosystems (Foster City, CA). Hes1 probes and primers were used as previously described (1-3). Quantitation for fold-change was performed by the standard curve method or the ΔΔCt method.

Cell Growth Assay. MTS assay was used to measure GBM cell growth as described previously (1-3). In short, 5000 GBM cells were plated in each well of a 48-well plate for the assay, and each reaction was set up in triplicate for each time-point. The CellTiter one solution MTS reagent (Promega, Madison, WI) was added to the culture according to the manufacturer's instruction. Absorbance at 490 nm was measured with a BioTek EL-800 plate reader after 1 h incubation at 37 °C. For NOTCH ligand treatment, recombinant rat JAG1/Fc chimera (catalog #599-JG) and recombinant human DLL1/Fc chimera (catalog #1818-DL) were purchased from R&D Systems (Minneapolis, MN). For co-culture experiments, GBM neurosphere cells seeded with GFP-labeled endothelial cells were sorted by flow cytometery (GFP-negative population) and plated into 48-well plates for the MTS assay as described above.

Soft Agar Clonogenic Assay. Pre-coating of a 6-well plate with 1% agarose was achieved by diluting sterile 4% agarose (Invitrogen) in DMEM. 5000 cells were then mixed with 0.5% agarose in the culture medium and laid on top of the 1% agarose layer in each well. Once

solidified, the cell-agarose mix was submerged in the growth medium, and the medium was replenished every 3 days. The plates were maintained for 3-4 weeks until visible spheres were formed, then stained with 0.5% Wright's stain (Sigma) in PBS for 1 hour at 37 °C, and imaged with a ChemiDoc machine (BioRad). The number of colony in each well was counted with QuantityOne software (BioRad) (1-3).

Immunoblotting. Protein was extracted from cells with the RIPA buffer (Pierce, Rockford, IL) containing protease inhibitors (Roche, Indianapolis, IN). Concentrations of protein lysates were determined by the BCA assay, using BSA as a standard (Pierce). 20-40 μg of protein were separated on 4-12% bis-tris mini-gels under reducing condition by electrophoresis and transferred to a 0.45-μm nitrocellulose membrane (Whatman) using XCell mini-cell and blot module kit (Invitrogen). Non-specific binding sites on the membrane were blocked with 5% non-fat dry milk in PBS with 0.01% Tween-20 (PBS-T) for 1h. Primary antibody dilutions were made in PBS-T (with or without 5% milk) and incubated with the membrane overnight at 4°C. HRP-linked secondary antibodies (Pierce) were diluted 1:2500 in PBS-T with 5% milk and incubated with the blot for 1h at room temperature. Protein of interest on the membrane was detected by enhanced chemiluminescence reaction (Pierce) then exposure to X-ray films (1-3). Primary antibodies and their dilutions used in immunoblotting were CD133 (Cell Signaling, 3663, 1:2,000), CD31 (Cell Signaling, 3528, 1:10,000), JAG1 (Cell Signaling, 2155, 1:2,000), DLL1 (Cell Signaling, 2588, 1:750), DLL4 (Cell Signaling, 2589, 1:750), Hes1 (generous gift from T. Sudo, Toray Industries, Inc., Japan, 1:2,000), PCNA (Cell Signaling, 2586, 1:100,000), β-actin (Sigma, A2223, 1:100,000), and GAPDH (Fitzgerald, RDI-TRK5G4-6C5, 1:1,000,000).

MRI. In vivo MRI studies were performed at the University of Michigan Molecular Imaging Core Facility (http://www.med.umich.edu/msair/index.htm). All mice were anesthetized with 2% isoflurane/air mixture throughout MRI examination. Mice lay supine, head first in a 7.0-Tesla Varian MR scanner (183-mm horizontal bore, Varian, Palo Alto, CA) with the body temperature maintained at 37 °C, using forced heated air. A double-tuned volume radiofrequency coil was used to scan the head region of the mice. Axial T2-weighted images were acquired using a fast spin-echo sequence with the following parameters: repetition time (TR)/effective echo time (TE), 4000/60 ms; echo spacing, 15 ms; number of echoes, 8; field of view (FOV), 20x20 mm; matrix, 256x128; slice thickness, 0.5 mm; number of slices, 25; and number of scans, 1 (total scan time ~2.5 min.). Tumor volumes were calculated from the MRI scans of the brain, using the voxel size.

Flow Cytometry. Flow cytometry analysis and cell sorting were performed at the core facility at the University of Michigan. Tumor regions from mouse brains were resected and mechanically dissociated into small pieces. Single cell dissociation was achieved by digestion with the PDD buffer (0.01% papain, 0.1% dispase II, 0.01% DNase I, 12.4 mM $MgSO_4$ in HBSS). Cells obtained were resupsended in PBS containing 0.5% BSA and 2 mM EDTA for analysis and sorting. H-2k^b antibody was utilized to differentiate between mouse and human cells, and CD31 antibody was used to detect endothelial cells. Cell viability was accessed by 7-AAD staining (BD Bioscience, 559925). Antibodies and their dilutions used for flow cytometry were CD133 (Miltenyi Biotec, AC-133 & 293C3, 1:10), H-2k^b (BD Bioscience, 553570, 1:10), and CD31-FITC (BD Bioscience, 555446, 1:5).

Immunofluorescence. Mouse brain tumor samples (from 4%-paraformaldehyde intracardiacally-perfused mice) and primary tumor samples from patients were fixed in 4% paraformaldehyde overnight at 4 °C, cryoprotected with 30% sucrose saturation, and cryoembedded in Tissue-Tek OCT. Tissue sections (8-µm thick) were permeablized (if required) with 0.4% Triton X-100 for 25 min at room temperature and blocked with 5% BSA in PBS for 30 min at room temperature. Samples were incubated with primary antibodies overnight at 4°C and secondary antibodies were applied for 1h at room temperature. Immunofluoresence slides were mounted with anti-fade prolong gold (Invitrogen) and imaged under an Olympus BX-51 fluorescence microscope (1-3). Primary antibodies and dilutions used for immunofluorescence were JAG1 (Cell Signaling, 2155, 1:100), DLL1 (Santa Cruz, sc-9102, 1:50), DLL4 (R&D Systems, MAB1389, 1:50), CD31 (Cell Signaling, 3528, 1:500), CD15 (Cell Signaling, 4744, 1:150), Ki-67 (NovoCastra, NCL-Ki67p, 1:500), cleaved caspase-3 (Cell Signaling, 9661, 1:250), NOTCH1 (University of Iowa Hybridoma Bank, bTAN 20, 1:20), NOTCH2 (University of Iowa Hybridoma Bank, C651.6DbHN, 1:10), HES5 (Santa Cruz, sc-13859, 1:50), NESTIN (Millipore, MAB5326, 1:1000), and human nuclei (Millipore, MAB1281, 1:500). Secondary antibodies used were Cy2-, Cy3-, AlexaFluor 488-, or AlexaFluor 568-conjugated and diluted to 1:200 (Cy2) or 1:500 (Cy3 and AlexaFluor) for the procedure. Cy-conjugated antibodies were obtained from JacksonImmunoResearch (West Grove, PA) and AlexaFluor-conjugated antibodies were purchased from Invitrogen.

References:

1. Fan X, Khaki L, Zhu TS, Soules ME, Talsma CE, Gul N, et al. NOTCH pathway blockade depletes CD133-positive glioblastoma cells and inhibits growth of tumor neurospheres and xenografts. Stem Cells. 2010 Jan;28(1):5-16.
2. Fan X, Matsui W, Khaki L, Stearns D, Chun J, Li YM, et al. Notch pathway inhibition depletes stem-like cells and blocks engraftment in embryonal brain tumors. Cancer Res. 2006 Aug 1;66(15):7445-52.
3. Fan X, Mikolaenko I, Elhassan I, Ni X, Wang Y, Ball D, et al. Notch1 and notch2 have opposite effects on embryonal brain tumor growth. Cancer Res. 2004 Nov 1;64(21):7787-93.

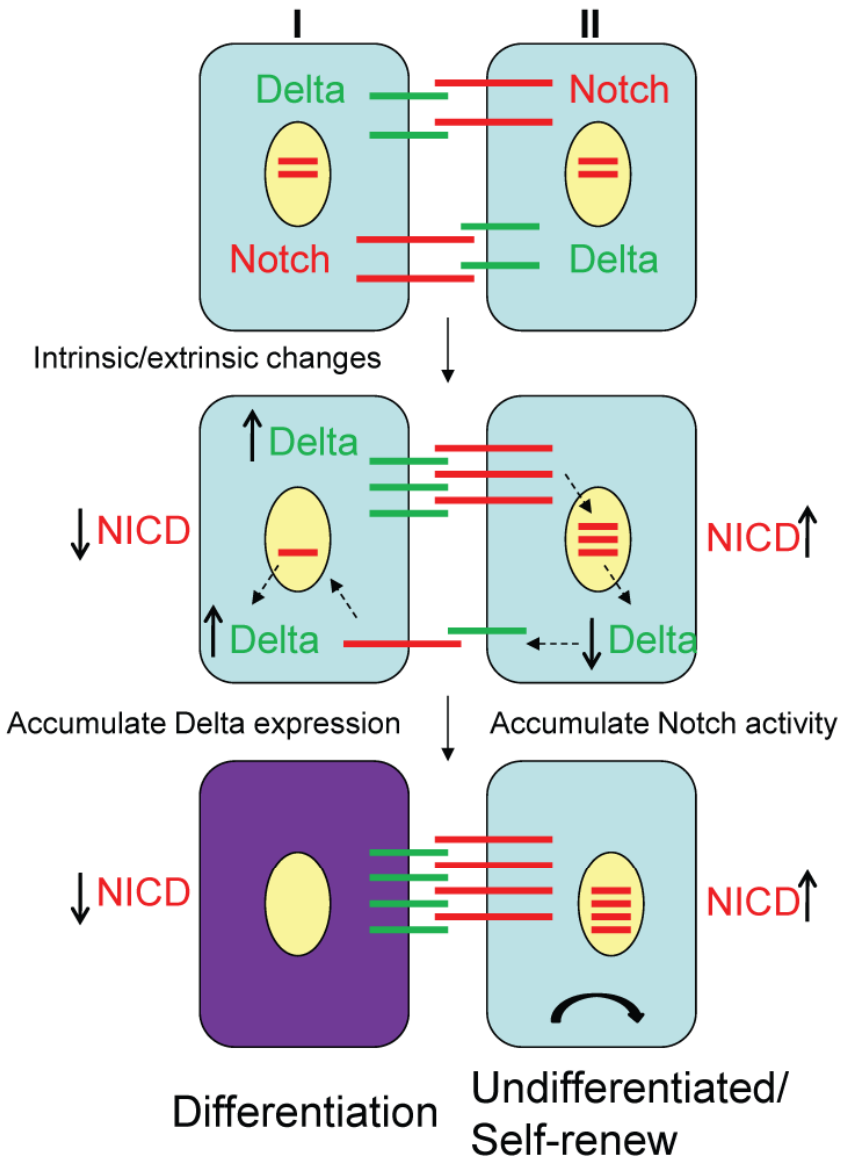

Figure S1: Lateral specification mediated by the Notch signaling pathway: During normal development, cell I and cell II (can be stem/progenitor cells) are derived from the same parental cell and express the same level of Notch ligand Delta and receptor Notch. Due to intrinsic and extrinsic changes, expression of Delta ligand is induced in cell I, which results in cell I sending more Delta ligands to bind Notch receptors expressed in cell II. Then the Notch activity in cell II is increased, which inhibits Delta ligand expression in cell II. The reduced Delta expression in cell II leads to a sending of less ligand from cell II to I, which results in decreased Notch activity in cell I. Decreased Notch activity in cell I renders more Delta ligand expressed in cell I. Finally, when the Notch activity in cell I is low enough, cell I will undergo differentiation and by expressing a higher level of Delta ligand to activate Notch signaling in cell II to keep cell II in undifferentiated stage (stem cell state) or self-renewal. This phenomenon is called lateral specification. In the CNS, cell I undergoes neuronal differentiation, whereas cell II remains the neural stem cell state to self-renew.

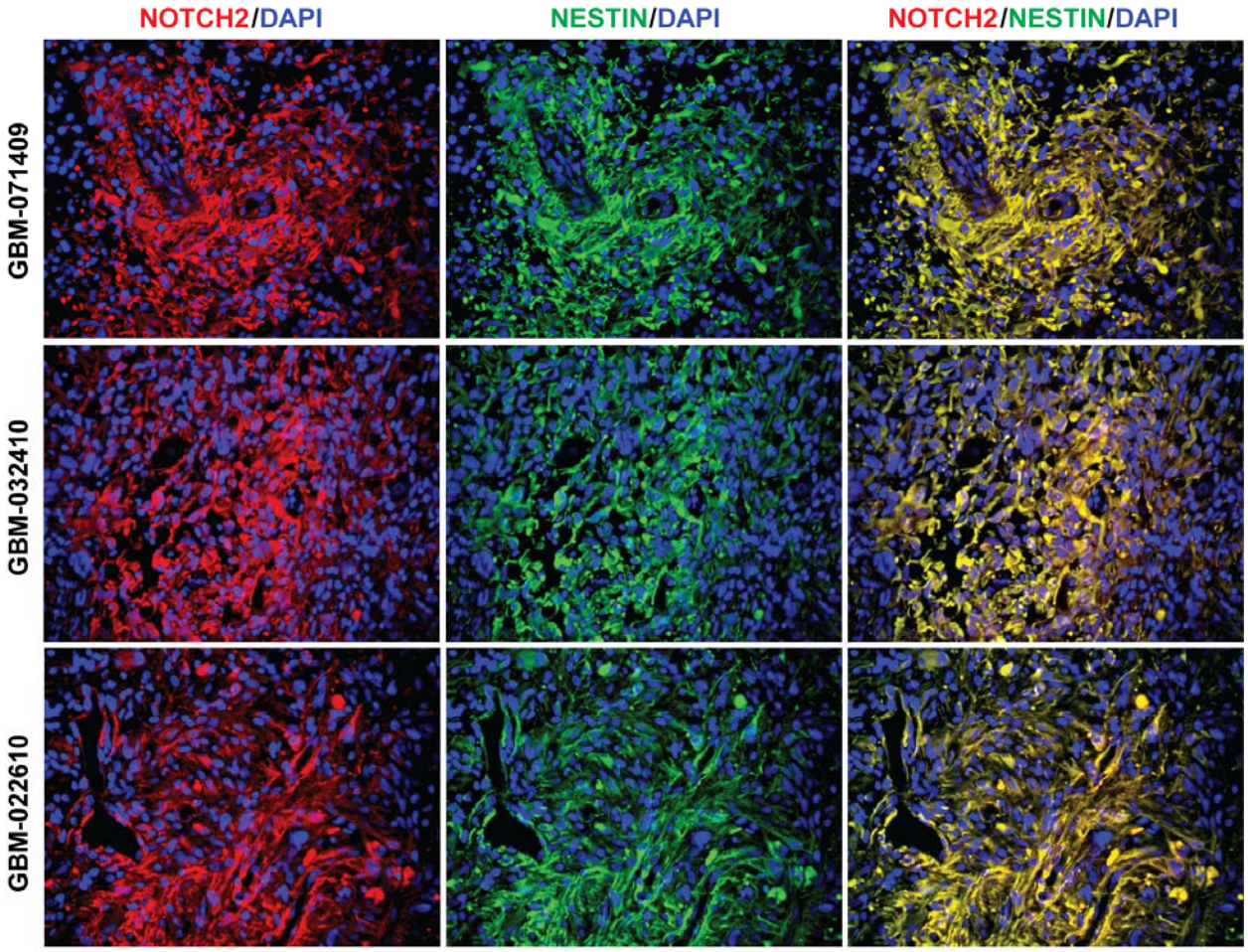

Figure S2: Expression of NOTCH2 and NESTIN are co-localized in the same cells in the primary GBM tumors: Frozen sections of three different primary GBM samples (GBM 071409, GBM-032410, and GBM 022610) were stained with anti-NOTCH2 (red) and anti-NESTIN (green) antibodies. DAPI is to stain the nuclei. Merged images show that expression of NOTCH2 and NESTIN was co-localized in the same cells within the tumor.

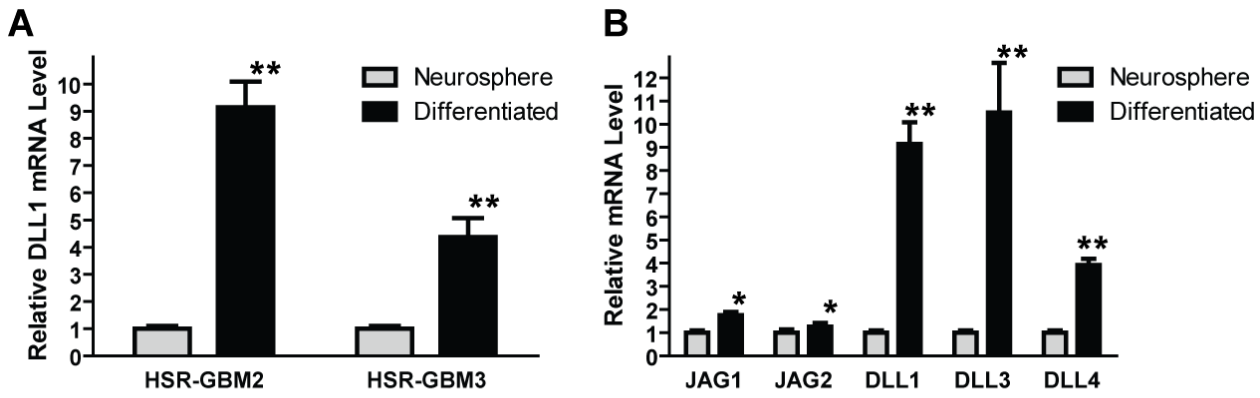

Figure S3: NOTCH ligand expression is induced in differentiatied GBM cells compared to GBM neurospheres. (A) mRNA expression of NOTCH ligands was quantified by qPCR. DLL1 is up-regulated in differentiated tumor cells compared GBM neurospheres (HSR-GBM1, HSR-GBM2, and HSR-GBM3). (B) In HSR-GBM2 neurosphere line, all the NOTCH ligands (DLL1, DLL3, DLL4, JAG1, and JAG2) were induced in differentiated tumor cells compared to GBM neurospheres. (n=3 repeats of each experiment, *: $p<0.05$, **: $p<0.01$, t-test, error bar represent s.e.m.)

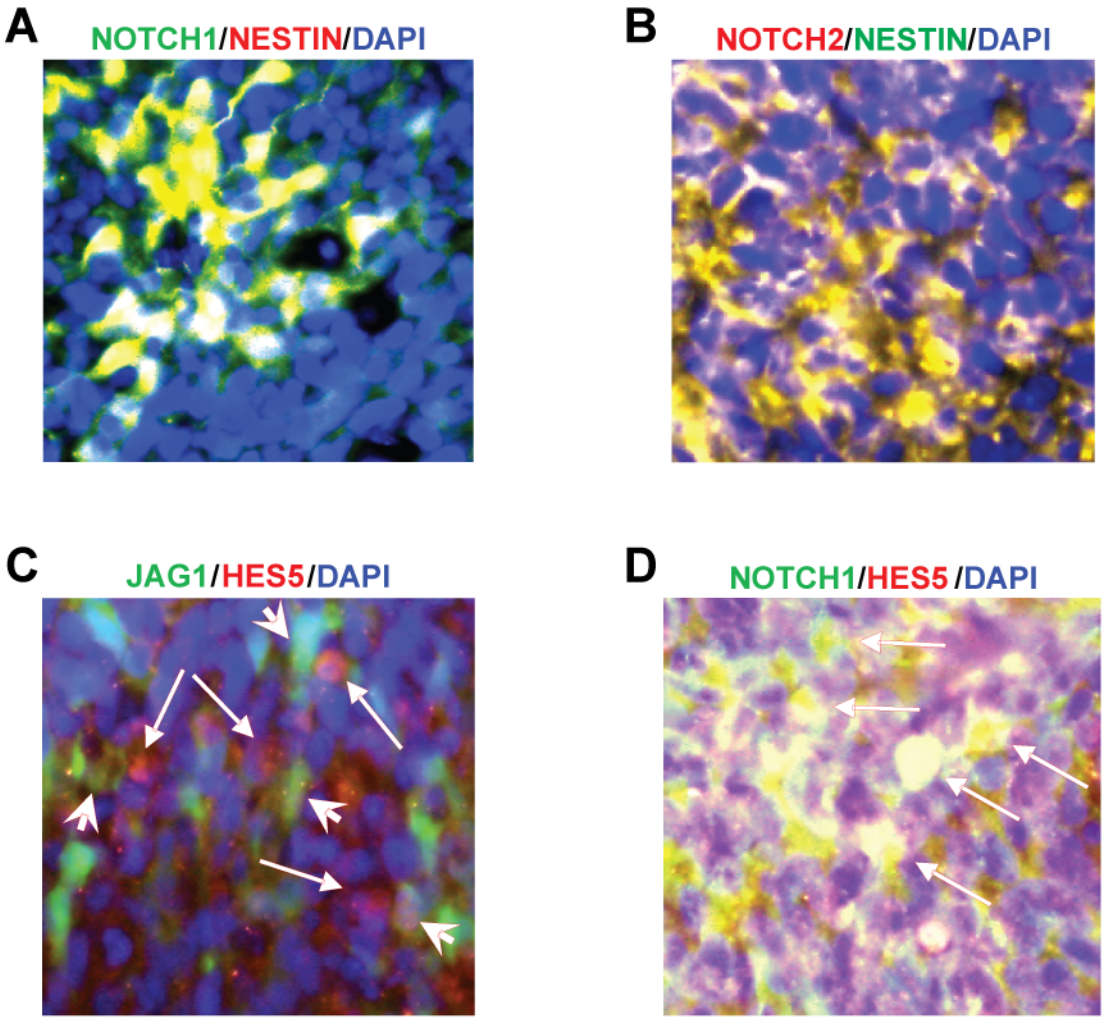

Figure S4: GBM intracranial xenografts mirror tumors in patients. (A) Expression of NOTCH1 and NESTIN was co-localized in the same cells in HSR-GBM1 intracranial xenograft: Frozen sections of HSR-GBM1 intracranial xenografts were stained with anti-NOTCH1 (green) and anti-NESTIN (red) antibodies. DAPI was to stain the nuclei. Merged images show that expression of NOTCH1 and NESTIN was co-localized in the same cells within the tumor. (B) Frozen sections of HSR-GBM1 intracranial xenografts were stained with anti-NOTCH2 (red) and anti-NESTIN (green) antibodies. DAPI was to stain the nuclei. Merged images show that expression of NOTCH2 and NESTIN was co-localized in the same cells within the tumor. (C) JAG1-expressing cells (green, arrowhead) were adjacent to HES5-expressing cells (red, arrow) in HSR-GBM1 intracranial xenografts. (D) NOTCH1-expression was co-localized with HES5-expression (arrow) in HSR-GBM1 intracranial xenografts.

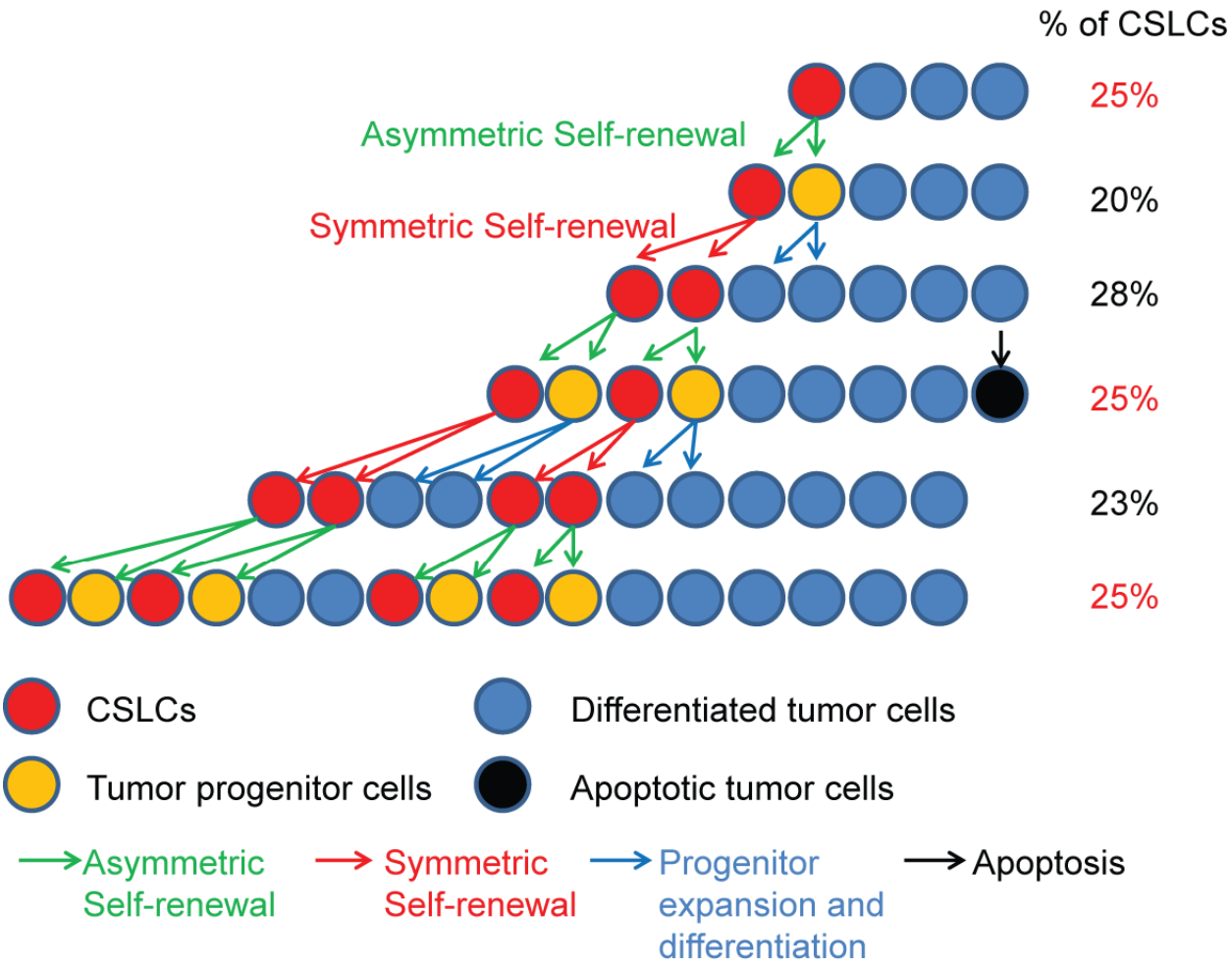

Figure S5: Schematic showing the cancer stem cells hypothesis: The CLSCs regenerate tumor tissue through symmetric and asymmetric self-renewal to maintain stable percentage of CSLC population within a tumor (using ~ 25% as an example), which is different from the model that each tumor cell can divide into two daughter cells.

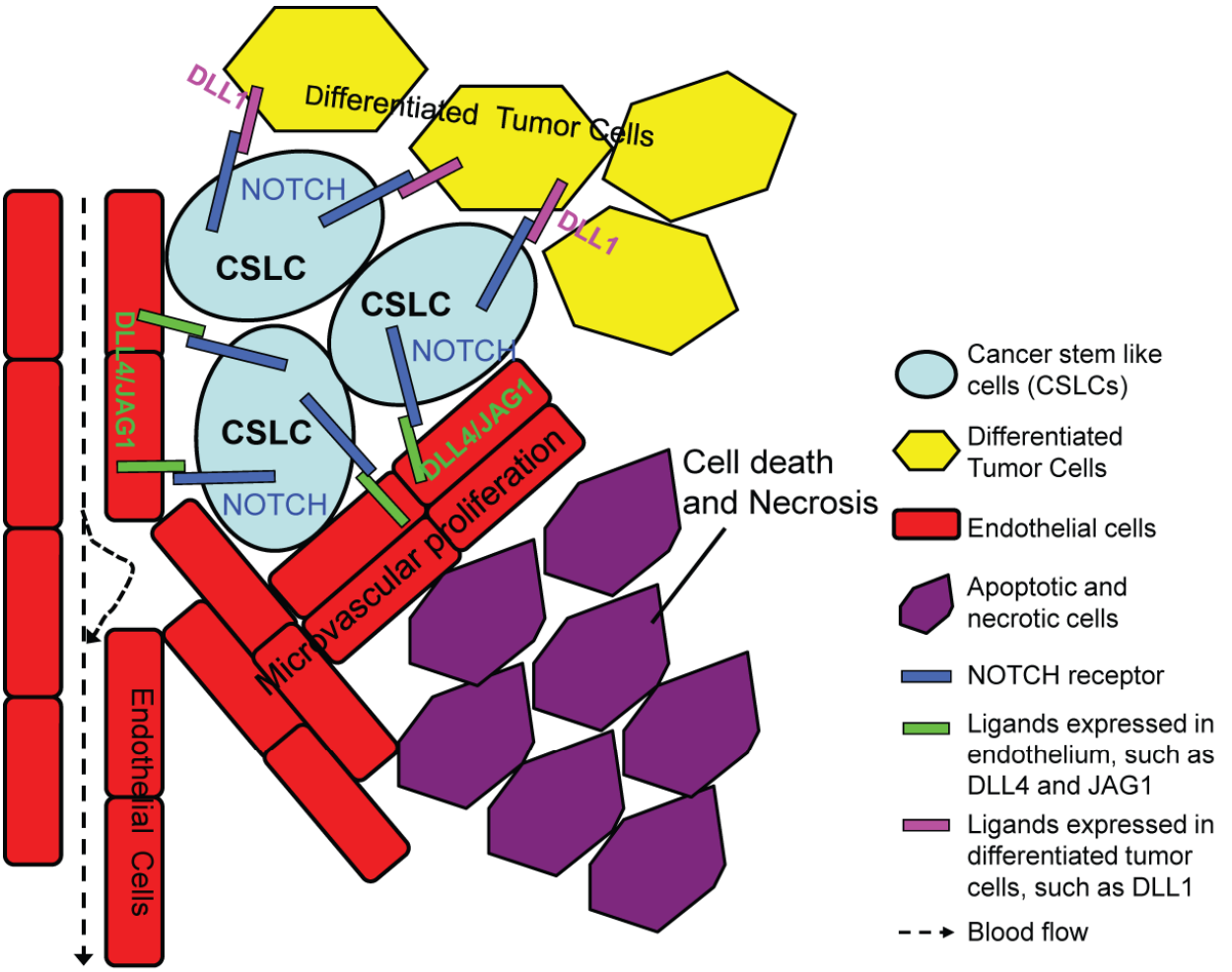

Figure S6: Model of endothelial cells and differentiated cells function as a niche for GBM CSLCs: Microvascular proliferation is the diagnosis hall-mark of GBM and GBM CSLCs have been found residing within the endothelial niche to self-renew. In the current study, we found that endothelial cells function as a niche to provide NOTCH ligand DLL4 and JAG1 to the NOTCH receptors expressed in adjacent CSLCs to activate NOTCH signaling in CSLCs. Differentiated tumor cells also function as a niche, but provide different NOTCH ligand, such as DLL1, to GBM CSLCs. Accumulating evidence shows that blocking signaling pathways that are required for CSLC self-renewal can target CSLCs, which generally reside around the microvascular proliferation region near the necrosis area (pseudopalisading necrosis), and are resistant to chemo- and radiation-therapy. However, as microvascular proliferating cells cannot form functional lumen-like structures, chemotherapeutic drugs or CSLC-targeting reagents may not be able to reach CSLCs which reside within such hypoxic endothelial niche. Here we show that the NOTCH ligands expressed in these microvascular endothelial cells can provide the ligand to the NOTCH receptors expressed in CSLCs to activate the NOTCH signaling pathway in CSLCs to self-renew. These data suggest that GBM CSLC depletion could be enhanced by blocking the interaction between endothelial cells and CSLCs, or by addition of agents that can eliminate endothelial niche in order to expose GBM CSLCs to the therapeutic agents.